Bone marrow-derived endothelial progenitor cells are a major determinant of nascent tumor neovascularization

Daniel J. Nolan, Alessia Ciarrocchi, Albert S. Mellick, et al.

Genes Dev. 2007 21: 1546-1558
Access the most recent version at doi:10.1101/gad.436307

Bone marrow-derived endothelial progenitor cells are a major determinant of nascent tumor neovascularization

Daniel J. Nolan,[1,4] Alessia Ciarrocchi,[2] Albert S. Mellick,[1] Jaspreet S. Jaggi,[3] Kathryn Bambino,[1] Sunita Gupta,[1] Emily Heikamp,[1] Michael R. McDevitt,[3] David A. Scheinberg,[3] Robert Benezra,[2] and Vivek Mittal[1,5]

[1]Cancer Genome Research Center, Cold Spring Harbor Laboratory, Woodbury, New York 11797, USA; [2]Program in Cancer Biology and Genetics, Memorial Sloan-Kettering Cancer Center, New York, New York 10021, USA; [3]Program in Molecular Pharmacology and Chemistry, Memorial Sloan-Kettering Cancer Center, New York, New York 10021, USA; [4]Graduate Program in Genetics, Stony Brook University, Stony Brook, New York 11794, USA

Tumors build vessels by cooption of pre-existing vasculature and de novo recruitment of bone marrow (BM)-derived endothelial progenitor cells (EPCs). However, the contribution and the functional role of EPCs in tumor neoangiogenesis are controversial. Therefore, by using genetically marked BM progenitor cells, we demonstrate the precise spatial and temporal contribution of EPCs to the neovascularization of three transplanted and one spontaneous breast tumor in vivo using high-resolution microscopy and flow cytometry. We show that early tumors recruit BM-derived EPCs that differentiate into mature BM-derived endothelial cells (ECs) and luminally incorporate into a subset of sprouting tumor neovessels. Notably, in later tumors, these BM-derived vessels are diluted with non-BM-derived vessels from the periphery, which accounts for purported differences in previously published reports. Furthermore, we show that specific ablation of BM-derived EPCs with α-particle-emitting anti-VE-cadherin antibody markedly impaired tumor growth associated with reduced vascularization. Our results demonstrate that BM-derived EPCs are critical components of the earliest phases of tumor neoangiogenesis.

[*Keywords*: Bone marrow transplantation; tumor angiogenesis; endothelial progenitor cells; endothelial cells; VE-cadherin; neovascularization]

Supplemental material is available at http://www.genesdev.org.

Received April 5, 2007; revised version accepted April 30, 2007.

The angiogenic switch involves the formation of new blood vessels (neovasculature), and is a hallmark of cancer emergence and progression (Folkman 1971; Hanahan and Folkman 1996; Carmeliet and Jain 2000). In adults, neovasculature formation relies on the sprouting and cooption of proliferating endothelial cells (ECs) from adjacent pre-existing host vasculature. More recent investigations suggest that the adult bone marrow (BM) is a source of cells that contributes significantly to postnatal angiogenesis (Carmeliet 2005; Kopp et al. 2006). Of the BM-derived cells, much focus has been directed on the proangiogenic hematopoietic mural cells that are recruited to the perivascular sites within the tumor bed (Coussens and Werb 2002; Pollard 2004; Carmeliet 2005; Kopp et al. 2006). Several populations of BM-derived hematopoietic cells have been reported to contribute to tumor angiogenesis. These include tumor-associated macrophages (TAMs) (Lin et al. 2001; Pollard 2004), Tie2-expressing monocytes (TEMs) (De Palma et al. 2005), VEGF receptor 1 (VEGFR1)-positive myeloid progenitors (Lyden et al. 2001), recruited BM-derived circulating cells (Grunewald et al. 2006), PDGFR$^+$ pericyte progenitors (Song et al. 2005), vascular leukocytes (Conejo-Garcia et al. 2005), and infiltrating neutrophils (Nozawa et al. 2006). Despite the general importance of these cells in tumor angiogenesis, the precise composition of specific individual lineages remains poorly understood.

In addition to the perivascular contribution of BM-derived hematopoietic cells, it has been proposed that the BM-derived endothelial progenitor cells (EPCs) provide an alternative source of ECs that contributes to neovessel formation (Lyden et al. 2001; Urbich and Dimmeler 2004; Khakoo and Finkel 2005; Kopp et al. 2006). In response to tumor cytokines, including VEGF (Asahara et al. 1999), putative VEGFR2-positive EPCs mobilize into the peripheral blood circulation to become circulating endothelial progenitors (CEPs), which subsequently move to the tumor vascular bed and incorporate into neovessels (Lyden et al. 2001; Rafii et al. 2002). The ex-

[5]**Corresponding author.**
E-MAIL mittal@cshl.edu; FAX (516) 422-4109.
Article is online at http://www.genesdev.org/cgi/doi/10.1101/gad.436307.

istence of a BM reservoir of EPCs, and their selective involvement in neovascularization, has attracted considerable interest because these cells may represent a novel target for therapeutic intervention. However, since the first description of EPCs (Asahara et al. 1997), their identity and relative contribution to neovasculature formation has remained controversial. Extensive variability in EPC contribution to vessel formation has been described. For instance, contributions as high as 50% (Lyden et al. 2001; Garcia-Barros et al. 2003) to as low as 5%–20% (Machein et al. 2003; Rajantie et al. 2004; Peters et al. 2005)—and, in some cases, undetectable levels (De Palma et al. 2003, 2005; Voswinckel et al. 2003; Gothert et al. 2004; He et al. 2004; Ziegelhoeffer et al. 2004)—have been reported. Such conflicting reports can be ascribed to a limited analysis of the EPC phenotype in each study, and a lack of more definitive methods employed for distinguishing vessel incorporated BM-derived ECs and intimately associated perivascular cells. Yet another source of variability may arise from the analysis of specific tumor types (Ruzinova et al. 2003; Li et al. 2004), and stages of tumor progression. Irrespective of these variable reports, CEPs are being considered as useful surrogate markers for monitoring cancer progression, as well as for optimizing efficacy of anti-angiogenic therapies, such as anti-VEGFR2 antibody therapy (Bertolini et al. 2006).

Therefore, the aim of this study was to determine the phenotypic identity, precise spatial and temporal contribution, and functional role of BM-derived EPCs in tumor angiogenesis. The data from our analysis show that EPCs are recruited to the tumor periphery preceding vessel formation. EPCs differentiate into ECs and incorporate luminally into a subset of sprouting tumor neovessels in various tumors. Selective ablation of EPCs in vivo resulted in a marked delay in tumor growth associated with distinct vascular defects, thereby underscoring the functional relevance of these cells in the process of tumor neovascularization.

Results

Spatial and temporal contribution of BM-derived EPCs in the neovascularization of growing tumors

In order to determine the contribution of the BM-derived EPCs to the formation of tumor neovasculature, we performed a BM transplantation (BMT) experiment. To track BM-derived cells in vivo, GFP$^+$ BM cells were isolated from C57BL/6-Tg (ACTbEGFP) mice and transplanted into lethally irradiated age-matched, syngeneic, non-GFP recipients. Analysis of BM and peripheral blood (4 wk post-transplantation) showed >95% reconstitution of recipient hematopoiesis by the donor BM-derived GFP$^+$ transplanted progenitor cells (data not shown), indicating stable replacement of original host stem cell population by the donor cells. Next, the reconstituted mice were challenged with intradermal tumors such as Lewis lung carcinoma (LLC), B6RV2 lymphoma, or orthotopic implanted melanoma (Aozuka et al. 2004). In addition to being syngeneic to the host, tumor implantations allow precise staging during tumor growth and minimize variability between animals.

We first determined the contribution of BM-derived endothelial progenitors to early stages of LLC tumor growth. Tumors were isolated, cryosectioned, and immunostained for EC markers (CD31/PECAM, VE-cadherin, VEGFR2/flk1, endoglin, and VCAM), progenitor markers (Prominin I/AC133), and various hematopoietic lineage markers. As expected, many BM-derived GFP$^+$ cells were observed infiltrating the tumor bed. Interestingly, at early stages of tumor growth (days 4–6), we observed a marked recruitment of BM-derived GFP$^+$ cells expressing the endothelial marker VE-cadherin at the periphery (Fig. 1A, arrows). Noticeably, these GFP$^+$ VE-cadherin$^+$ cells were recruited to early tumors prior to vessel invasion from the neighboring host tissue (Fig. 1A). Although these cells expressed VE-cadherin, we determined that they were not mature ECs because they lacked typical mature EC morphology, expressed uniform cell surface VE-cadherin (cf. VE-cadherin localized at the adherens junctions between two adjacent mature ECs in a vessel), and expressed low CD31 (>10-fold reduction relative to ECs in vessels) (Fig. 1B, arrows; Supplementary Fig. S1A). Low CD31 expression on these cells was further confirmed by flow cytometric analysis of early tumors (Supplementary Fig. S1B). These cells also expressed the endothelial-specific marker VEGFR2, endoglin, and progenitor cell marker Prominin I/AC133 (Supplementary Fig. S2A–C), representing EPCs. Indeed, some of these markers have been used in defining EPCs previously (Asahara et al. 1997; Peichev et al. 2000; Ribatti 2004; Kopp et al. 2006). The EPCs lacked expression of all hematopoietic lineage markers tested, including CD11b (monocytes, subsets of lymphocytes, Dendritic cells, and NK cells), CD45RB (monocytes, granulocytes, and subsets of T and B cells), and CD41 (megakaryocytes) (Supplementary Fig. S3A–C). Dim CD45 expression was observed in EPCs in the BM compartment but not in the tumors (data not shown). These results are consistent with a published report that VE-cadherin$^+$ progenitor cells in the adult BM do not contribute to the hematopoietic lineages (Kim et al. 2005). In summary, these results demonstrate that BM-derived EPCs are recruited to early tumors prior to vessel formation, and that the EPCs are distinct from the hematopoietic lineages.

BM-derived ECs luminally incorporate into early tumor neovessels

We next determined the contribution of BM-derived EPCs to neovessel formation in early vascular LLC tumors (days 6–8). These early vascular tumors were characterized by the presence of CD31$^+$ neovessels of various sizes (Fig. 2A). A subset of these nascent sprouting vessels contained incorporated BM-derived GFP$^+$ CD31$^+$ VE-cadherin$^+$ cells (Fig. 2A, arrows). High-resolution microscopic analysis of these chimeric vessels showed that the vessel-incorporated BM-derived cells exhibited

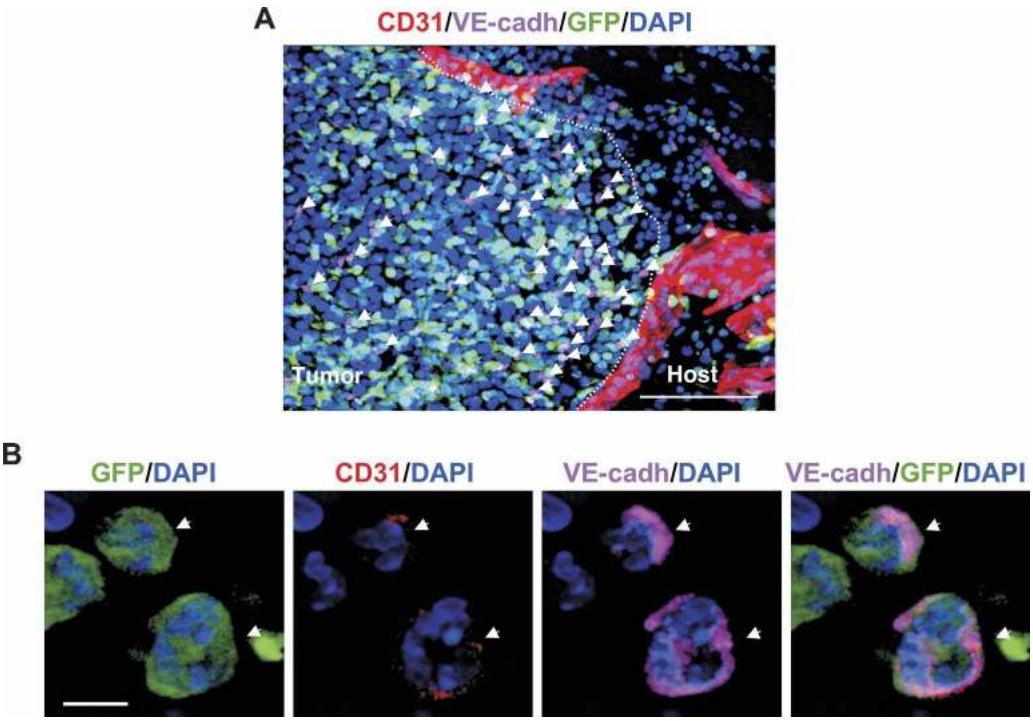

Figure 1. BM-derived EPCs are recruited at the periphery of early tumors. (*A*) A representative fluorescent image showing recruitment of BM-derived GFP$^+$ VE-cadherin$^+$ EPCs (arrows) at the periphery of early nonvascularized LLC tumors (days 4–6; $n = 15$). CD31$^+$ mature vessels are observed in the host tissue but not in the tumors. The dotted line separates the host tissue from the tumor. Bar, 100 µm. (*B*) High-resolution image showing GFP$^+$ VE-cadherin$^+$ CD31^{low} EPCs (arrows) at the periphery of LLC tumors (day 4). DAPI was used to stain the nucleus of all cells. Bar, 5 µm.

hallmarks of a mature EC such as spindle-like morphology, high surface CD31 expression, and characteristic VE-cadherin staining at the intercellular adherens junctions (Fig. 2B). Optical sectioning (Z-stack resolution of 0.275 µm) further confirmed that the BM-derived ECs had a single nucleus, and that the GFP and CD31 signals were localized to the same individual cell (Fig. 2C; Supplementary Fig. S4A), indicating that the incorporated EC was derived from the BM. Computer three-dimensional (3D) rendering analysis confirmed that the VE-cadherin staining was shared between the GFP$^+$ BM-derived EC and the non-BM-derived EC in these vessels (data not shown). High-resolution microscopy also allowed us to exclude false positives comprised of perivascular GFP$^+$ cells intimately associated with vessels (Supplementary Fig. S4B,C), suggesting that low-resolution light microscopy may lead to the overestimation of luminally incorporated BM-derived ECs, as reported previously (Lyden et al. 2001; Garcia-Barros et al. 2003). It is worth noting that under all circumstances, BM-derived ECs were found in chimeric vessels with non-BM-derived ECs as opposed to vessels comprised exclusively of BM-derived ECs. The BM-derived GFP$^+$ ECs also lacked expression of hematopoietic lineage markers including CD11b (data not shown) and CD45 as determined by both immunostaining of tumor sections and flow cytometry (Supplementary Fig. S5A–C). BM-derived EPCs and vessel-incorporated ECs were also observed during early growth phase of other tumors, including melanomas (Supplementary Fig. S6A,B) and B6RV2 lymphoma (data not shown). Taken together, these results demonstrate that in response to a tumor challenge, BM-derived EPCs, which are distinct from proangiogenic hematopoietic cells, are first recruited to early tumors followed by luminal incorporation of BM-derived ECs into the neovessels.

We next performed flow cytometric analysis to determine the relative numbers of BM-derived EPCs (GFP$^+$ VE-cadherin$^+$ CD31^{low} CD11b$^-$) and non-BM-derived ECs (GFP$^-$ VE-cadherin$^+$ CD31^{high} CD11b$^-$) at different stages of tumor growth (Fig. 3A). BM-derived EPCs comprised of 25%–35% of the total ECs in the early phases of tumor growth (days 4–6), and this contribution decreased about fourfold in late tumors (day 14), consistent with histological analysis (data not shown). Notably, in late tumors there was an enhanced recruitment of local non-BM-derived GFP$^-$ ECs (65%–75%, days 10–14), which diluted the observed contribution of BM-derived EPCs. We next quantified luminally incorporated BM-derived ECs in tumor vessels. Vessel counts from optically sectioned tumors showed that ~20% of vessels had incorporated BM-derived ECs (GFP$^+$ VE-cadherin$^+$ CD31$^+$) at day 6 (Fig. 3B), and these chimeric vessels markedly decreased with time (<1% remaining after 4 wk). As an alternate approach to quantify luminal incorporation, we performed systemic perfusion with fluorescently labeled isolectin GS-IB$_4$, which stains specific carbohydrates on ECs (Laitinen et al. 1987). Analysis of tumor vessels with

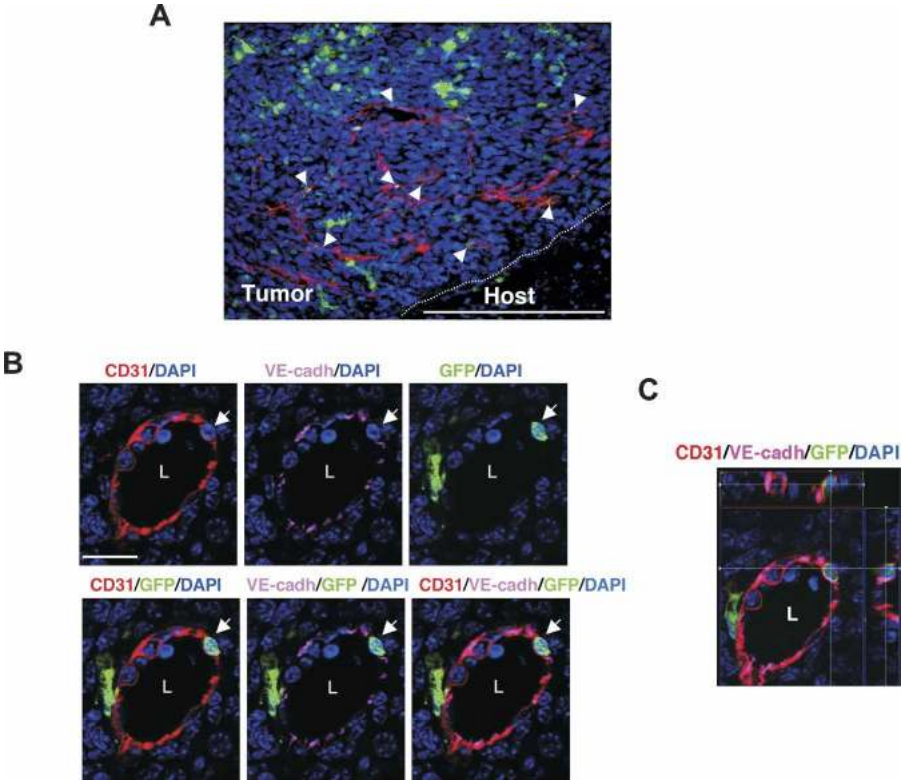

Figure 2. BM-derived ECs are luminally incorporated in tumor neovasculature. (*A*) Representative fluorescent image showing CD31$^+$ mature vessels in LLC tumors (days 6–8; $n = 15$). Arrows depict incorporated BM-derived ECs in these vessels. Bar, 200 µm. The dotted line separates the host tissue from the tumor. (*B*) High-resolution image of a representative blood vessel showing an incorporated mature BM-derived GFP$^+$ CD31$^+$ VE-cadherin$^+$-coexpressing cell (arrow). The lumen of the vessel (L) and VE-cadherin staining the adherens junctions between ECs are shown. Bar, 20 µm. (*C*) Optical sectioning (Z-stack resolution, 0.275 µm) of the BM-derived ECs showing that GFP and CD31 signals are localized within the same individual cell (*X–Z*- and *Y–Z*-axes are represented by the *top* and side panels).

anti-CD31 antibody showed that isolectin GS-IB$_4$ staining was confined to the functional vessels (Supplementary Fig. S7A) as compared with choleratoxin, which leaked into the surrounding tumor tissue (Supplementary Fig. S7B). Furthermore, fluorescent isolectin specifically stained the luminal surface of endothelial cells in vessels (Fig. 3C, arrow), and these cells could be detected by flow cytometric analysis (Fig. 3D, top-right quadrant). We therefore used flow cytometric analysis to determine the percentage of luminally incorporated BM-derived ECs in the tumor neovasculature. Of the total functional vasculature, as determined by Lectin$^+$ CD31$^+$ CD11b$^-$ cells, 31% (±8.3) of the luminal ECs (GFP$^+$ Lectin$^+$ CD31$^+$ CD11b$^-$) in day 6 LLCs (Fig. 3E) are BM derived. A similar kinetic analysis performed in a melanoma model also showed recruitment of EPCs prior to vessel infiltration, early contribution of BM-derived ECs, and their subsequent dilution by host ECs (Supplementary Fig. S6; data not shown). A comparison of the contribution of BM-derived EPCs and ECs in different tumors is summarized in Supplementary Table S1.

Together, these results demonstrate that BM-derived EPCs are recruited to early avascular tumors. EPCs differentiate into ECs and luminally incorporate into a subset of sprouting peripheral vessels from the host. This is followed by massive invasion of peripheral vasculature into the tumor mass, diluting the BM-derived vessels at late stages of tumor growth.

BM-derived EPCs contribute to spontaneous tumors

In order to confirm that these events are also taking place in spontaneous tumors, we performed a similar analysis in breast tumors arising in MMTV-PyMT transgenic mice (Guy et al. 1992). In these animals, the PyMT oncogene is expressed under the transcriptional control of the mouse mammary tumor virus promoter/enhancer specifically in the mammary epithelium (Guy et al. 1992). The PyMT transgene activates pathways similar to that induced by ErbB2 (Desai et al. 2002), and, importantly, this murine tumor model recapitulates human breast cancer progression from early nonmalignant hyperplasia (~6 wk of age) and adenoma (8–9 wk of age), to early and late malignant adenocarcinoma (8–12 wk of age) (Lin et al. 2003).

We examined the contribution of BM-derived EPCs and luminally incorporated ECs at various stages of these mammary tumors developing in animals previ-

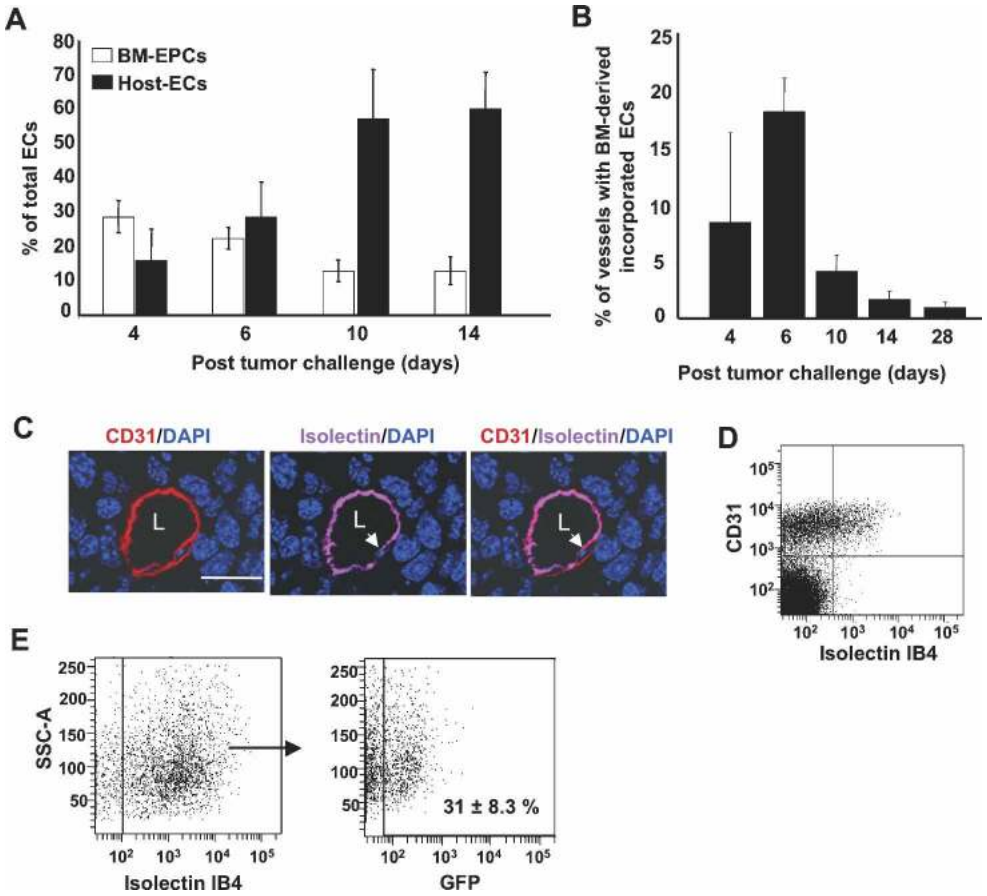

Figure 3. Contribution of BM-derived EPCs and ECs as a function of tumor progression. (*A*) Flow cytometry analysis of LLC tumors (days 4–14; $n = 5$ per group), showing relative contribution of BM-derived EPCs (GFP$^+$ VE-cadherin$^+$ CD31^{low}, CD11b$^-$), and host-derived ECs (GFP$^-$ VE-cadherin$^+$ CD31$^+$, CD11b$^-$). Total number of cells analyzed was 2×10^5 per animal, except for day 4, due to smaller tumor size. Each analysis was performed in duplicate. Error bars represent standard deviations. This experiment was repeated three times, and identical trends were observed. (*B*) Quantification of vessels in LLC tumors (days 4–28) with incorporated BM-derived ECs (GFP$^+$, CD31$^+$, VE-cadherin$^+$), a minimum of 400 vessels counted per time point from six nonsequential sections, and 20 images per tumor (Z-stacks evaluated for each section). Error bars represent standard deviations. (*C*) A representative image showing a tumor vessel from an animal perfused with isolectin GS-IB4 and stained with CD31. Arrows indicate isolectin IB4 staining the luminal surface of the EC in the vessel. (L) Lumen. Bar, 20 µm. (*D*) Flow cytometric analysis of LLC tumors (days 6–8) showing that fluorescent isolectin specifically stains a population of luminally incorporated CD31$^+$ ECs. (*E*, *left*) Flow cytometric analysis showing that fluorescent isolectin stains a population of luminally incorporated ECs (CD31$^+$ CD11b$^-$) derived from LLC tumors. (*Right*) Of these, 31% ± 8.3% are BM derived (GFP$^+$ CD31$^+$ Isolectin$^+$ CD11b$^-$). The averages and standard deviation were determined by analyzing 1×10^5 cells per animal ($n = 5$). (SSC-A) Side scatter values.

ously transplanted with GFP$^+$ BM. Early adenomas (~8 wk of age) were identified as closely packed multifocal acini surrounded by pre-existing host vessels (Fig. 4A, arrows). Adenomas at this stage had not yet recruited neovasculature from the pre-existing vessels, and very few GFP$^+$ BM cells were observed infiltrating the adenoma mass (Fig. 4A). A subset of adenomas progressing into early carcinoma showed foci of BM-derived GFP$^+$ cells including EPCs (Fig. 4B, arrows). Such foci of BM-derived cell infiltration have been previously observed in adenomas (Lin et al. 2003). Analysis of early carcinomas (10 wk of age) showed high density of BM infiltration and increased vessel density. These vascular tumors were characterized by the presence of CD31$^+$ neovessels of various sizes (Fig. 4C). These sprouting nascent vessels had incorporated BM-derived GFP$^+$ CD31$^+$ ECs (Fig. 4C). In this model, quantitation of luminally incorporated BM-derived ECs by flow cytometry was technically challenging due to the closely packed, multifocal nature of breast tumor development. We therefore performed vessel counts by microscopy of early carcinomas, which showed that ~5%–10% of host vessels had incorporated BM-derived GFP$^+$ ECs (GFP$^+$ VE-cadherin$^+$ CD31$^+$) (Fig. 4E).

The observation that BM-derived EPCs precede host ECs and that BM-ECs contribute to neovascularization in early stages of breast tumor progression is consistent with that observed in transplanted tumors, highlighting the general relevance of these cells in tumor neovascularization.

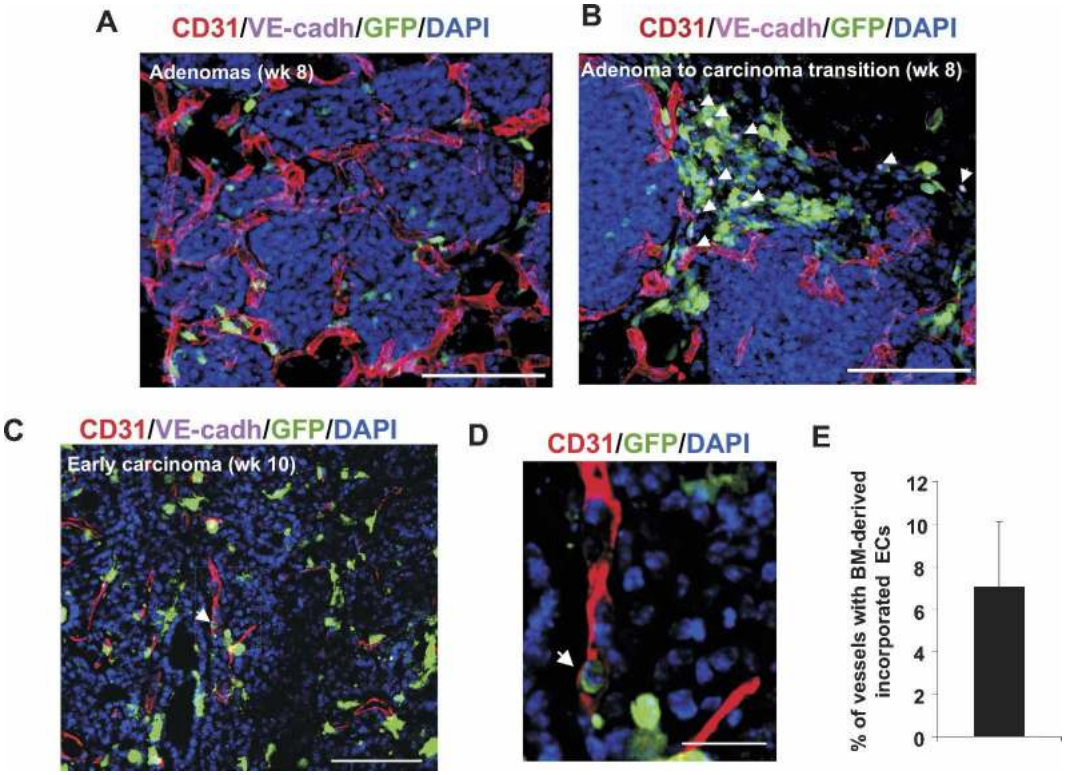

Figure 4. Contribution of BM-derived EPCs in spontaneous breast tumors. (*A*) Primary adenoma lesions in mammary gland sections from a PyMT mouse at 8 wk of age. Pre-existing CD31$^+$ vessels are observed surrounding the adenomas. Bar, 100 µm. (*B*) Recruitment of BM-derived GFP$^+$ VE-cadherin$^+$ EPCs (arrows) at the periphery of the avascular adenoma–carcinoma progression is shown. Bar, 100 µm. (*C*) An early carcinoma showing recruited CD31$^+$ mature vessels in the tumor mass (10 wk of age). Arrow depicts incorporated BM-derived ECs in a vessel. Bar, 100 µm. (*D*) High-resolution image of a representative blood vessel (box in *C*) showing an incorporated mature BM-derived GFP$^+$ CD31$^+$-coexpressing cell (arrow). Bar, 20 µm. DAPI was used to stain the nucleus of all cells. (*E*) Quantification of vessels in breast tumors (10 wk old) with incorporated BM-derived ECs (GFP$^+$ CD31$^+$ VE-cadherin$^+$). A minimum of 250 vessels were counted from nonsequential sections from four animals, and Z-stacks were evaluated for each section. Error bars represent standard deviations.

BM-derived EPCs differentiate into ECs and incorporate into vessels

We next sought to formally demonstrate that BM-derived EPCs have the potential to differentiate into mature ECs and incorporate into neovessels. First, we sorted GFP$^+$ EPCs (Lin$^-$ VE-cadherin$^+$) from the BM by flow cytometry (Fig. 5A), and cocultured them with spontaneously immortalized murine ECs, mHEVc (Cook-Mills et al. 1996), in matrigel. Notably, mHEVcs in culture have lost CD31 and VE-cadherin expression, but have retained VCAM expression (Cook-Mills et al. 1996). By 12 h, VE-cadherin$^+$ EPCs had not differentiated into ECs and remained VCAM-negative (Fig. 5B). However, by day 2, GFP$^+$ BM-ECs that had incorporated into the growing vascular networks were detected (Fig. 3D, top panel). These incorporated GFP$^+$ BM-derived ECs expressed VCAM (Fig. 5C, bottom panel) and CD31 (Supplementary Fig. S8A). High-resolution microscopy confirmed that the incorporated EC was indeed derived from the GFP$^+$ EPC (Supplementary Fig. S8B). We next determined whether the EPCs recruited to early tumors differentiated into ECs and incorporated into neovessels. GFP$^+$ VE-cadherin$^+$ CD11b$^-$ cells were flow sorted from early tumors (day 4) (Fig. 5D). EPCs identified as CD31^{low} (as depicted in Supplementary Fig. S1B), were cocultured with mHEVcs in matrigel. By day 2, GFP$^+$ EPCs had differentiated into GFP$^+$ ECs and incorporated into the vascular networks (Fig. 5E). In contrast, GFP$^+$ CD11b$^+$ hematopoietic cells isolated from the same early tumors neither differentiated into ECs nor incorporated into vessels (Fig. 5F). Collectively, these results demonstrate that BM-derived VE-cadherin$^+$ EPCs contribute to the endothelial lineage.

Specific ablation of EPCs results in defects in angiogenesis-mediated tumor growth

To determine if the BM-derived EPCs had a functional role in angiogenesis-mediated tumor growth, we selectively ablated EPCs with an anti-VE-cadherin antibody, E4G10. The monoclonal antibody E4G10 specifically recognizes the exposed monomeric epitope on the immediate N terminus of VE-cadherin, which becomes masked upon *trans*-dimerization in mature ECs in ves-

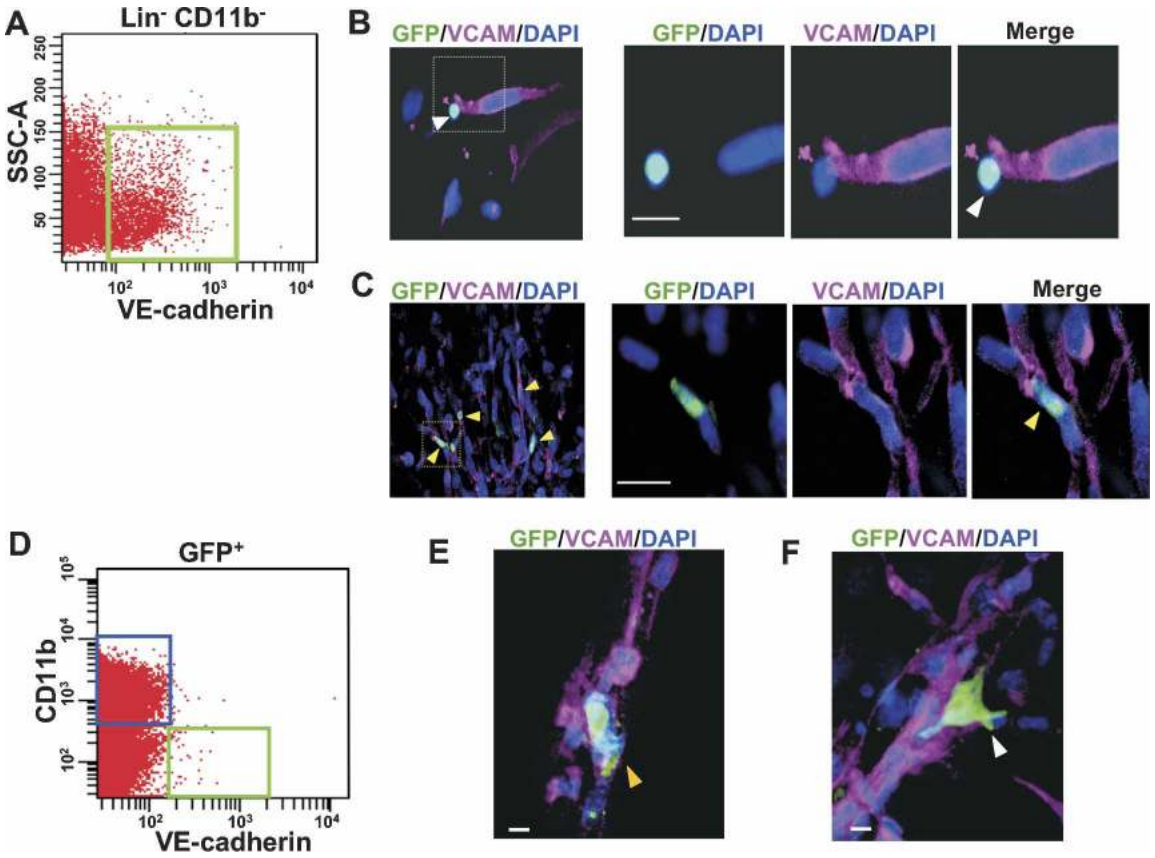

Figure 5. BM-derived EPCs differentiate into mature ECs and incorporate into vascular networks. (*A*) Scatter plot showing VE-cadherin-expressing EPCs in the BM-derived Lin$^-$ CD11b$^-$ fraction (green box). (*B*) Immunostaining of cocultured BM-derived GFP$^+$ EPCs and mature ECs (non-GFP) in 3D matrigel at 12 h. (*Right* panels) A high-resolution image showing an unincorporated, BM-derived GFP$^+$ VCAM$^-$ EPC (white arrow). (*C*) Multiple BM-derived ECs (GFP$^+$ VCAM$^+$, yellow arrows) that have incorporated into vascular tubes 48 h following coculture. (*Right* panels) A high-resolution image showing an incorporated BM-derived GFP$^+$ EC (yellow arrow). (*D*) Scatter plot showing GFP$^+$ cells from day 4 LLC tumors. GFP$^+$ VE-cadherin$^+$ CD11b$^-$ EPCs (green box) and GFP$^+$ VE-cadherin$^-$ CD11b$^+$ hematopoietic cells (blue box) were live-sorted. (*E*) Immunostaining of the cocultured BM-derived GFP$^+$ EPCs sorted in *D* and mature ECs (non-GFP) in 3D matrigel at 48 h. High-resolution microscopy showing an incorporated BM-derived GFP$^+$ VCAM$^+$ EC (yellow arrow). (*F*) Immunostaining of the cocultured GFP$^+$ CD11b$^+$ hematopoietic cells sorted in *D* and mature ECs (non-GFP) in 3D matrigel at 48 h. High-resolution microscopy showing an unincorporated BM-derived GFP$^+$ VCAM$^-$ cell (white arrow). Bars, 10 µm. (SSC-A) Side scatter values.

sels (May et al. 2005). Thus, E4G10 allows targeting of monomeric VE-cadherin present on EPCs, but not the dimerized form present in vessel incorporated ECs. We confirmed that E4G10 recognizes VE-cadherin only on the EPCs, but not in mature ECs comprising the nascent early tumor neovessels (Fig. 6A, white arrows; Supplementary Fig. S9), compared with a pan-VE-cadherin antibody 11D4.1 (VE-cadh^{pan}) that recognized both the monomeric VE-cadherin on EPCs and homodimerized VE-cadherin on ECs in vessels (Fig. 6A, red arrows). In addition, the VE-cadherin epitope was exposed in neither the luminally incorporated BM-derived GFP$^+$ ECs (data not shown) nor the EC projections of sprouting nascent vessels in early tumors (Fig. 6B,C).

The cytotoxic potency of E4G10 was enhanced by coupling the antibody to an α-particle-emitting isotope, actinium-225 (^{225}Ac) (McDevitt et al. 2001), so that target cells could be effectively killed at low concentrations of the antibody. Administration of ^{225}Ac-labeled E4G10 (50 nCi, 0.6 µg antibody per administration per animal) reduced accumulated LLC tumor burden per animal by ~50% (day 14, $P = 0.001$) compared with the administration of equivalent amounts of ^{225}Ac-labeled IgG isotype control mixed with unlabeled E4G10 (Fig. 7A). The impaired tumor growth was associated with a marked reduction in EPC contribution (>45%, $P = 0.004$) as determined by flow cytometry (Fig. 7B) and confirmed by histology (Supplementary Fig. S10). Ablation of VE-cadherin$^+$ cells was specific, since no detectable change was observed in other BM-derived GFP$^+$ infiltrating cell populations, including the CD11b$^+$ hematopoietic cells available in the immediate proximity ($P = 0.86$) (Fig. 7C). Notably, ablation of VE-cadherin$^+$ EPCs resulted in a 40% reduction in BM-derived luminally incorporated ECs (GFP$^+$ CD31$^+$ Isolectin$^+$ CD11b$^-$) ($P = 0.016$) (data not shown), and a dramatic reduction in vessel density

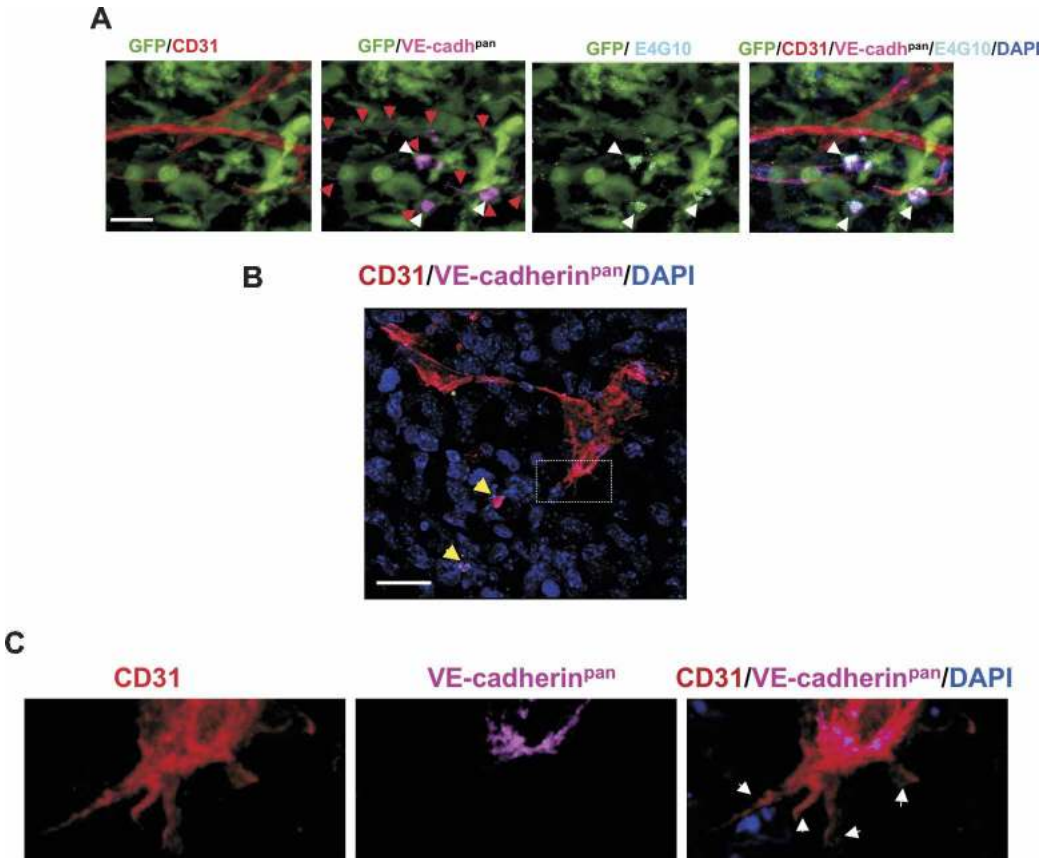

Figure 6. VE-cadherin monoclonal antibody E4G10 specifically recognizes EPCs and not mature ECs. (*A*) Five-color immunostaining of early LLC tumors (day 6) with VE-cadherin antibody E4G10 (white arrows), pan-VE-cadherin antibody 11D4.1 (VE-cadh^{pan}, red arrows), and CD31. E4G10 exclusively staining EPCs is shown (double red and white arrows). Bar, 20 µm. (*B*) Immunostaining of early tumors (day 6) with CD31 and a pan-VE-cadherin antibody. Low-magnification image showing endothelial projections of the invading tumor vasculature. Yellow arrows depict VE-cadherin$^+$ EPCs in the vicinity. Bar, 20 µm. GFP staining is not included for precise visualization. (*C*) Higher magnification of the area denoted by a rectangle in *B*, showing that the endothelial projections are devoid of VE-cadherin (white arrows).

($P = 0.006$) in later tumors (Fig. 7D,E). No gross or histopathological toxicity was observed in normal tissues or their vasculature at the dosage administered (data not shown). Taken together, these results suggest that ablation of EPCs results in marked delay in tumor growth associated with decreased vessel density.

Discussion

In this study, we provide evidence that BM-derived EPCs, as defined by the cell surface expression of VE-cadherin, VEGFR2, CD31^{low}, Endoglin, and Prominin I/AC133 (Supplementary Table S2), differentiate into mature ECs and contribute both structurally and functionally to tumor neoangiogenesis. Further analysis demonstrated that the EPCs are distinct from other hematopoietic and proangiogenic BM-derived cell types such as TEMs (De Palma et al. 2005), macrophages (Pollard 2004), recruited BM-derived circulating cells (Grunewald et al. 2006), pericyte progenitors (Song et al. 2005), and infiltrating neutrophils (Nozawa et al. 2006). The BM-derived ECs are also distinct from vascular leukocytes (Conejo-Garcia et al. 2005), because they do not express leukocyte marker CD45 (Supplementary Fig. S5).

Analysis of multiple tumor types showed that EPCs differentiate into mature ECs and luminally incorporate into neovessels, clearly demonstrating the derivation of tumor vasculature from transplanted BM cells. A systematic kinetic analysis showed that EPCs are recruited to the tumor periphery preceding vessel formation, and are luminally incorporated into a subset of sprouting tumor neovessels. Noticeably, these chimeric BM-derived vessels were eventually diluted with host-derived vessels, thereby explaining the low contribution observed by other investigators in large, established tumors (De Palma et al. 2003, 2005; Gothert et al. 2004; Rajantie et al. 2004; Larrivee et al. 2005; Duda et al. 2006). Possibly, de Palma et al. (2003) were unable to detect BM-derived tumor ECs not only due to the analysis of late tumors (4 wk), but also because the Tie2 promoter in their study does not mark all the Tie2$^+$ mature ECs or bona fide EPCs. In their study, the reporter GFP gene was not driven by the endogenous Tie2 promoter. Instead, the

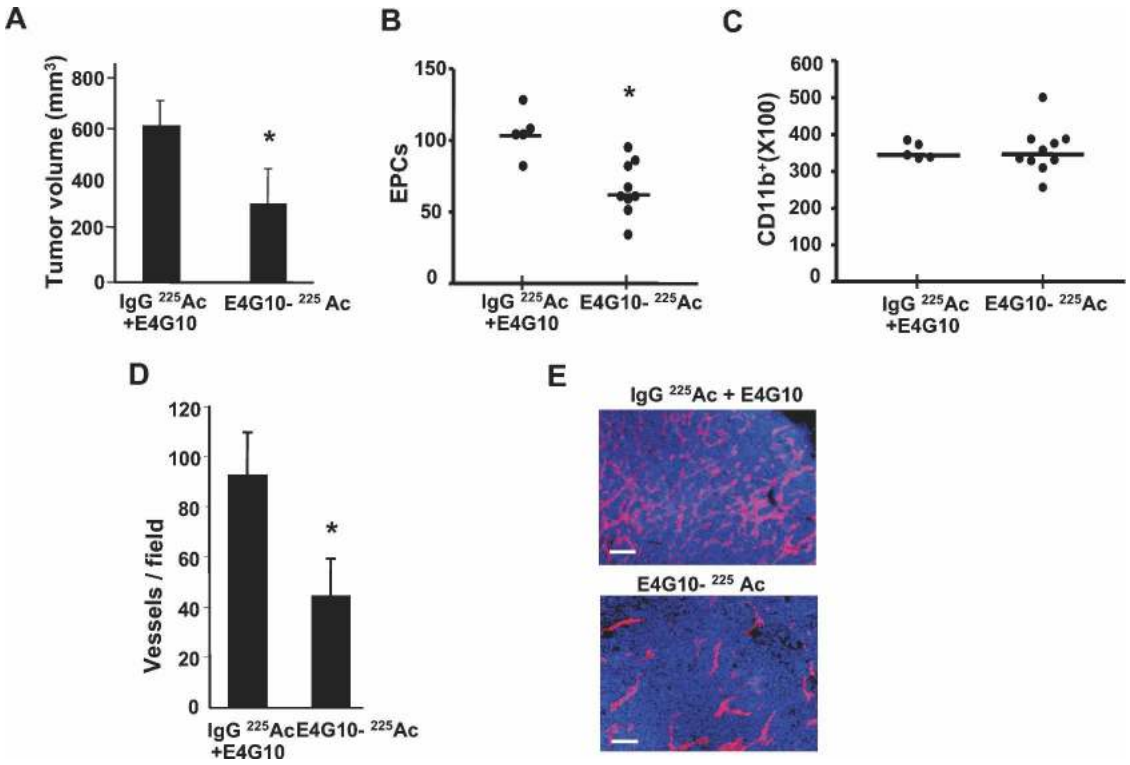

Figure 7. Selective ablation of EPCs results in delayed tumor growth in vivo. (*A*) LLC tumor volume at day 14 in animals administered with isotype control ^{225}Act-IgG and unlabeled E4G10 or ^{225}Act-E4G10 antibody (n = 5, 10 per group, respectively). (*B*) Number of BM-derived EPCs (GFP$^+$ VE-cadherin$^+$ CD31^{low} CD11b$^-$) cells in early tumors (day 6) in animals administered with control or ^{225}Act-E4G10 antibody at day 3 and 5 post-tumor innoculation (n = 5, 10, respectively; 1×10^5 events counted per n). Bars denote averages. (*C*) BM-derived GFP$^+$ CD11b$^+$ cells in tumors from animals treated as in *B* (n = 5, 10, respectively; 1×10^5 events counted per n). Bars denote averages. (*D*) Vessel density in tumors in animals treated with control and test antibody (day 14; n = 5, 7 per group, respectively) (*E*) CD31 immunostaining of tumor sections (day 14) isolated from E4G10-treated and control-treated animals. Bar, 50 μm. Error bars represent standard deviations. (*) Significant by t-test; $P < 0.05$.

Tie2 promoter driving the GFP gene was introduced by a lentiviral construct into murine embryonic stem cells. Therefore, it is possible that random integration of lentiviral vectors may have failed to identify the true repopulating EPCs. In a similar study, using an endothelial-specific (SCL) inducible Cre recombinase to activate a stop-floxed β-galactosidase gene, Gothert et al. (2004) argue the lack of BM-precursor contribution to the tumor endothelium. The SCL promoter does not mark the progenitors in the BM, but was used to identify BM-derived cells that mature in the periphery. The lack of LacZ$^+$ peripheral vessels observed at 14 d post-implantation is in agreement with our data that BM-derived chimeric vessels are diluted by mature peripheral vessels in later tumors.

Our results differ from those of Garcia-Barros et al. (2003), and Lyden et al. (2001), who reported 50%–90% BM-derived CD31$^+$ vessels in large established tumors as estimated by X-gal staining in LacZ$^+$ BM transplants. Possibly, X-gal detection by light microscopy may impose difficulty in reliably distinguishing vessel-incorporated ECs from closely associated perivascular cells, resulting in overestimation of BM-derived vessels. Since these reports were published, the use of high-resolution confocal microscopy for the accurate determination of vessel incorporated ECs has been advocated (De Palma et al. 2003; Larrivee et al. 2005). Indeed, in this study we have demonstrated that 3D high-resolution microscopy is required to accurately discern luminally incorporated ECs from perivascular cells (Supplementary Fig. S4B,C). Our data are in disagreement with those of Spring et al. (2005), who showed derivation of BM-derived neovessels as a late event in carcinogenesis. In these studies, flow cytometric analysis of CD31$^+$ GFP$^+$ cells does not provide a reliable measure of vessel-incorporated BM-derived ECs. Luminal incorporation by flow cytometry can be more reliably quantitated in the context of specific isolectin administration and analysis of Isolectin$^+$ CD31$^+$ GFP$^+$ CD11b$^-$ cells (Fig. 3). GFP determines BM derivation, isolectin ensures luminal incorporation, CD31 confirms ECs, and CD11b gates out any hematopoietic contribution in the CD31 channel. This approach is critical because CD31 is also expressed by a subset of hematopoietic cells (Baumann et al. 2004), and therefore the use of CD31 alone provides an unreliable measure of bona fide ECs.

Evidence for the contribution of EPCs to ischemic revascularization resulting from severe vascular injury has

been reported both in humans and mice. For example, Minami et al. (2005) have shown that circulating ECs engraft luminally into 15%–29% of the vessels of the transplanted heart in patients with sex-mismatched heart transplants. These data suggest that during acute vascular injury, the demand for neoangiogenesis increases to a point where there is a profound contribution of circulating host-derived ECs to neoangiogenesis. Similarly, during the angiogenic switch, as it may occur in the early phases of tumor growth, the rapid demand for neoangiogenesis may facilitate the recruitment of BM-derived EPCs, as observed in our investigation. The presence of EPCs in tumors prior to recruitment of host vasculature raises the possibility that the BM-derived EPCs may play a critical role in initiating the recruitment of non-BM-derived vessels to the tumors. At this stage, EPC differentiation and luminal incorporation of BM-derived EC may be necessary for providing structural support and guidance to these nascent vessels. Deciphering the mechanisms governing the dynamic interactions between the BM-derived EPCs and non-BM ECs will require further investigations.

The specific recruitment to and association of EPCs with the neovasculature of both spontaneous and transplanted tumors in our studies highlight the general relevance of these cells in tumor angiogenesis. The functional significance of EPCs in angiogenesis-mediated tumor growth was determined by their effective and selective ablation with a radiolabeled anti-VE-cadherin antibody. Strikingly, EPC ablation resulted in decreased vessel density and reduced tumor growth, suggesting that the contribution of BM-derived ECs is critical for angiogenesis-mediated tumor progression. To address the possibility that EPCs carrying the radioactive anti-VE-cadherin antibody may have destroyed other proangiogenic cells in *trans* via a bystander effect, we quantitated other cell types observed in the proximity of the EPCs. Radiolabeled E4G10 administration caused no detectable change in BM-derived GFP^+ infiltrating cells, including the $CD11b^+$ hematopoietic cells that are available in the immediate proximity. This result strongly argues against the possibility of a bystander effect. In addition, our data are in agreement with the notion that short-ranged α-emitting ^{225}Ac atoms are capable of killing individual cells with minimal collateral damage (McDevitt et al. 2001; Borchardt et al. 2003).

Interestingly, Lamszus et al. (2005) have shown that the administration of E4G10 on day 1 post-tumor challenge resulted in significant inhibition of angiogenesis and tumor growth. In contrast, administration of E4G10 during later tumor growth did not effect either vessel density or tumor growth, suggesting that the tumor phenotype resulted from blocking peak EPC contribution and not from targeting differentiated ECs in established vasculature, consistent with our data. Our results and interpretation of the specificity of E4G10 differ from those of Liao et al. (2002). In these studies, the authors showed that systemic administration of 1000 µg of fluorescent E4G10 (cf. 0.6 µg in our experiments) stained a subset of tumor vasculature. Perhaps excessive antibody administration in their experiments resulted in nonspecific binding to the permeable tumor vasculature and the tumor stroma. In our study, we clearly demonstrated that the VE-cadherin epitope is not exposed on invading nascent vessels in early tumors. Our observations are in agreement with various independently published reports demonstrating that VE-cadherin is rapidly internalized and degraded in proliferating/migrating ECs (Xiao et al. 2003; Lampugnani et al. 2006), and showing that VE-cadherin is not critical for the formation of nascent vasculature, but is required to maintain or prevent the disassembly of nascent blood vessels (Crosby et al. 2005). Possibly, the suppression of tumor growth observed by Liao et al. (2002) may have resulted as a result of EPC blockade, which the authors did not investigate.

The clinical implications of BM-derived ECs in angiogenesis-mediated tumor growth are further bolstered by their recent identification in the vasculature of human tumors (Peters et al. 2005). In this study of human sex-mismatched BM transplant recipients who later developed tumors, fluorescence in situ hybridization analysis showed that ~2%–12% of ECs infiltrating the tumors were derived from the BM (Peters et al. 2005). Perhaps, in these studies low BM-EC contribution was estimated due to analysis of rare archived late human tumor biopsies. Peters et al. (2005) may have missed the early peak contribution of BM-derived ECs in these late tumors. Thus, inhibition of the function of these EC progenitors, perhaps in combination with existing anti-angiogenic therapies, may provide a promising approach to blocking neoangiogenesis in rapidly growing tumors, rebounding tumors, or regrowing tumors following incomplete surgical removal of a primary lesion. Furthermore, as demonstrated recently, EPC targeting can also enhance the efficacy of other anti-cancer therapies, such as vascular disruptive agents (Shaked et al. 2006). Indeed, our ability to delay angiogenesis-mediated tumor growth by ablating BM progenitor cells identifies these cells as promising therapeutic targets.

Materials and methods

Cell lines and growth conditions

The murine lymphoma cell line B6RV2 (Lyden et al. 2001), LLC cell line LLCs/D122 (provided by Lea Eisenbach, Wiesmann Institute of Science, Rehovot, Israel), and melanoma cell line B16F0 (American Type Culture Collection) were used to generate tumors in C57BL/6 mice. LLCs and B16F0 were maintained in DMEM supplemented with 10% fetal bovine serum (FBS). B6RV2 cells were maintained in RPMI with 15% FBS. Murine ECs, mHEVc, were cultured as described (Cook-Mills et al. 1996; Tudor et al. 2000).

Spontaneous tumor model

Male PyMT mice (obtained from mouse models of human cancer consortium; NCI) on a FVB/N background were randomly bred with FVB/N females (Jackson Laboratories) lacking the PyMT transgene to obtain female mice heterozygous for the

PyMT transgene. These female carriers developed mammary tumors by 5–6 wk, which were staged according to Lin et al. (2003). All procedures involving mice were conducted in accordance with protocols reviewed and approved by the CSHL Animal Care and Use Committee.

BM isolation, Lin⁻ cell purification, and transplantation

GFP transgenics, C57BL/6-Tg (ACTbEGFP)10sb/J, or FVB.Cg-Tg (GFPU)5Nagy/J (The Jackson Laboratory), were used as the donor strain. In these strains, GFP is driven by a hybrid chicken β-actin promoter and cytomegalovirus intermediate early enhancer. BM cells were harvested by flushing the femurs and tibias of adult animals. Total BM cells (1×10^7) were transplanted into lethally irradiated (1100 rads) recipients. Lin⁻ cells were enriched using the Lineage Cell Depletion Kit (CD5, CD45R [B220], CD11b, anti-Ly-6G [Gr-1], 7-4, and Ter119 antibodies) and a magnetic separation device, MACS (Milteyni Biotech). The purity of the Lin⁻ fraction was determined using a fluorescent antibody specific for lineage-specific markers by flow cytometry. All animal protocols were reviewed and approved by the CSHL Animal Care and Use Committee.

Flow cytometry, tumor growth, immunohistochemistry, and microscopy

C57BL/6 mice were inoculated intradermally with 5×10^6 to 2×10^7 LLC/D122 or B6RV2 cells, or with 5×10^5 B16F0 cells, and tumor size was monitored (width × 0.5 length^2).

Tumors were excised from sacrificed animals, minced, and then digested for 45–60 min at 37°C with an enzyme cocktail (Collagenase A, elastase, and DNase I; Roche Applied Science), and filtered through a 30-µm strainer. Single-cell suspensions were preblocked with Fc block (CD16/CD32; BD Biosciences PharMingen) and then incubated with the following primary antibodies from Pharmingen: rat IgG2aκ and IgG2aβ isotype control; CD31/PECAM-1 (clone MEC 13.3); VE-cadherin/CD144 (clone 11D4.1); CD11b (clone M1/70.); VEGFR2/Flk1 (clone avas12α1). Labeled cell populations were measured by a LSRII flow cytometer (Beckton Dickenson); compensation for multivariate experiments was performed with FACS Diva software (Becton Dickinson Immunocytometry Systems). Flow cytometry analysis was performed using a variety of controls such as isotype antibodies, FMO samples (Perfetto et al. 2004), and unstained samples for determining appropriate gates, voltages, and compensations required in multivariate flow cytometry. Tumor-bearing mice were anesthetized and then perfused with phosphate buffer followed by 4% paraformaldehyde. In some cases, animals were injected with Alexa Fluor 647-conjugated isolectin GS-IB4 or Choleratoxin β subunit (50 µg for 10 min; Molecular Probes) prior to phosphate buffer perfusion. Tumors were incubated overnight in paraformaldehyde, followed by 20% sucrose, and were cryoembedded in Tissue-tek O.C.T. embedding compound (Electron Microscopy Sciences). Immunohistochemistry was performed using the primary antibodies Prominin1 (clone 13A4; eBiosciences), Endoglin (clone MJ7/18), CD45RB (clone 16A), pan-CD45 (clone 30-F11), CD41 (clone MWREQ30; BD Pharmingen), and E4G10 (ImClone), in addition to antibodies described for flow cytometry on 30-µm-thick sections. Usually, primary antibodies were directly conjugated to various Alexa Fluor dyes or Quantum Dots using antibody labeling kits (Inivtrogen) performed as per the manufacturer's instructions. In the case of Alexa Fluor 750, conjugations were performed using succinimidyl esters and purified over BioSpin P30 Gel (Bio-Rad). GFP-positive cells were detected by their own signal.

Fluorescent images of endothelium that contained donor-derived ECs were obtained using a computerized Zeiss fluorescent microscope (Axiovert 200M), fitted with an apotome and a HRM camera. Images were analyzed by using Axiovision 4.5 software. The average depth of the optical sections was 30 µm, with a resolution of 0.275–0.35 µm.

EPC differentiation assay

Total BM cells from GFP transgenic animals were first enriched for Lin⁻ cells as described before. Lin⁻ cells were incubated with VE-cadherin (Alexa Fluor 647) and CD11b (Alexa Fluor 750) antibodies. Using multivariate flow sorting, a pure GFP⁺ EPC population (VE-cadherin⁺ CD11b⁻) was collected by FACS Aria (BD Biosciences). Approximately 5000 EPCs were cocultured with 5×10^4 murine ECs, mHEVc (gift from J.M. Cook-Mills, University of Cincinnati, Cincinnati, OH) on matrigel (BD Biosciences) supplemented with Medium 200 and LSGS (Cascade Biologics). Similarly, EPCs (1×10^3) and hematopoietic cells (~5×10^4) were flow-sorted from early tumors (day 4) derived from GFP⁺ BMT animals and cocultured with 5×10^4 murine ECs. Low CD31 expression on EPCs was confirmed with a PE-conjugated CD31 antibody. Immunostaining was performed directly on matrigels with VCAM (clone 429, MVCAM.A; BD Pharmingen) and CD31/PECAM-1 (clone MEC 13.3) antibody after fixation with 4% paraformaldehyde.

Preparation and administration of radioimmunoconjugate

^{225}Ac (Oak Ridge National Laboratory) was conjugated to E4G10 (a gift from ImClone) using a two-step labeling method, as described (McDevitt et al. 2002; Borchardt et al. 2003). Radiopurity and immunoreactivity of the radioimmunoconjugate (RIC) were determined as described (Borchardt et al. 2003). Mice were anesthetized and injected intravenously with the RIC in 100 µL at days 3, 5, 8, and 12 (50 nCi, 0.6 µg antibody per administration).

Statistical analysis

Analysis of different treatment groups was performed using the Mann-Whitney *T*-test.

Acknowledgments

We thank Barry Burbach, Michael Hemann, Lea Eisenbach (LLC/D122), J.M. Cook-Mills (mHEVc ECs), Chad May (E4G10 antibody), Tim Tully, and Nishi Sinha (flow cytometry) for advice and reagents. We thank Zaher Nahle, Scott Powers, Scott Lowe, Greg Hannon, and members of the Mittal laboratory for comments on the manuscript. This work was supported by NIH grants to V.M. and R.B., and funding from the Robert I. Goldman foundation, Philip Morris USA, and the Berkowitch Foundation to V.M. A.C. is supported by an AICF fellowship.

References

Aozuka, Y., Koizumi, K., Saitoh, Y., Ueda, Y., Sakurai, H., and Saiki, I. 2004. Anti-tumor angiogenesis effect of aminopeptidase inhibitor bestatin against B16–BL6 melanoma cells orthotopically implanted into syngeneic mice. *Cancer Lett.* **216:** 35–42.

Asahara, T., Murohara, T., Sullivan, A., Silver, M., van der Zee, R., Li, T., Witzenbichler, B., Schatteman, G., and Isner, J.M. 1997. Isolation of putative progenitor endothelial cells for angiogenesis. *Science* **275:** 964–967.

Asahara, T., Takahashi, T., Masuda, H., Kalka, C., Chen, D., Iwaguro, H., Inai, Y., Silver, M., and Isner, J.M. 1999. VEGF contributes to postnatal neovascularization by mobilizing bone marrow-derived endothelial progenitor cells. *EMBO J.* **18:** 3964–3972.

Baumann, C.I., Bailey, A.S., Li, W., Ferkowicz, M.J., Yoder, M.C., and Fleming, W.H. 2004. PECAM-1 is expressed on hematopoietic stem cells throughout ontogeny and identifies a population of erythroid progenitors. *Blood* **104:** 1010–1016.

Bertolini, F., Shaked, Y., Mancuso, P., and Kerbel, R.S. 2006. The multifaceted circulating endothelial cell in cancer: Towards marker and target identification. *Nat. Rev. Cancer* **6:** 835–845.

Borchardt, P.E., Yuan, R.R., Miederer, M., McDevitt, M.R., and Scheinberg, D.A. 2003. Targeted actinium-225 in vivo generators for therapy of ovarian cancer. *Cancer Res.* **63:** 5084–5090.

Carmeliet, P. 2005. Angiogenesis in life, disease and medicine. *Nature* **438:** 932–936.

Carmeliet, P. and Jain, R.K. 2000. Angiogenesis in cancer and other diseases. *Nature* **407:** 249–257.

Conejo-Garcia, J.R., Buckanovich, R.J., Benencia, F., Courreges, M.C., Rubin, S.C., Carroll, R.G., and Coukos, G. 2005. Vascular leukocytes contribute to tumor vascularization. *Blood* **105:** 679–681.

Cook-Mills, J.M., Gallagher, J.S., and Feldbush, T.L. 1996. Isolation and characterization of high endothelial cell lines derived from mouse lymph nodes. *In Vitro Cell. Dev. Biol. Anim.* **32:** 167–177.

Coussens, L.M. and Werb, Z. 2002. Inflammation and cancer. *Nature* **420:** 860–867.

Crosby, C.V., Fleming, P.A., Argraves, W.S., Corada, M., Zanetta, L., Dejana, E., and Drake, C.J. 2005. VE-cadherin is not required for the formation of nascent blood vessels but acts to prevent their disassembly. *Blood* **105:** 2771–2776.

De Palma, M., Venneri, M.A., Roca, C., and Naldini, L. 2003. Targeting exogenous genes to tumor angiogenesis by transplantation of genetically modified hematopoietic stem cells. *Nat. Med.* **9:** 789–795.

De Palma, M., Venneri, M.A., Galli, R., Sergi, L.S., Politi, L.S., Sampaolesi, M., and Naldini, L. 2005. Tie2 identifies a hematopoietic lineage of proangiogenic monocytes required for tumor vessel formation and a mesenchymal population of pericyte progenitors. *Cancer Cell* **8:** 211–226.

Desai, K.V., Xiao, N., Wang, W., Gangi, L., Greene, J., Powell, J.I., Dickson, R., Furth, P., Hunter, K., Kucherlapati, R., et al. 2002. Initiating oncogenic event determines gene-expression patterns of human breast cancer models. *Proc. Natl. Acad. Sci.* **99:** 6967–6972.

Duda, D.G., Cohen, K.S., Kozin, S.V., Perentes, J.Y., Fukumura, D., Scadden, D.T., and Jain, R.K. 2006. Evidence for incorporation of bone marrow-derived endothelial cells into perfused blood vessels in tumors. *Blood* **107:** 2774–2776.

Folkman, J. 1971. Tumor angiogenesis: Therapeutic implications. *N. Engl. J. Med.* **285:** 1182–1186.

Garcia-Barros, M., Paris, F., Cordon-Cardo, C., Lyden, D., Rafii, S., Haimovitz-Friedman, A., Fuks, Z., and Kolesnick, R. 2003. Tumor response to radiotherapy regulated by endothelial cell apoptosis. *Science* **300:** 1155–1159.

Gothert, J.R., Gustin, S.E., van Eekelen, J.A., Schmidt, U., Hall, M.A., Jane, S.M., Green, A.R., Gottgens, B., Izon, D.J., and Begley, C.G. 2004. Genetically tagging endothelial cells in vivo: Bone marrow-derived cells do not contribute to tumor endothelium. *Blood* **104:** 1769–1777.

Grunewald, M., Avraham, I., Dor, Y., Bachar-Lustig, E., Itin, A., Yung, S., Chimenti, S., Landsman, L., Abramovitch, R., and Keshet, E. 2006. VEGF-induced adult neovascularization: Recruitment, retention, and role of accessory cells. *Cell* **124:** 175–189.

Guy, C.T., Cardiff, R.D., and Muller, W.J. 1992. Induction of mammary tumors by expression of polyomavirus middle T oncogene: A transgenic mouse model for metastatic disease. *Mol. Cell. Biol.* **12:** 954–961.

Hanahan, D. and Folkman, J. 1996. Patterns and emerging mechanisms of the angiogenic switch during tumorigenesis. *Cell* **86:** 353–364.

He, Y., Rajantie, I., Ilmonen, M., Makinen, T., Karkkainen, M.J., Haiko, P., Salven, P., and Alitalo, K. 2004. Preexisting lymphatic endothelium but not endothelial progenitor cells are essential for tumor lymphangiogenesis and lymphatic metastasis. *Cancer Res.* **64:** 3737–3740.

Khakoo, A.Y. and Finkel, T. 2005. Endothelial progenitor cells. *Annu. Rev. Med.* **56:** 79–101.

Kim, I., Yilmaz, O.H., and Morrison, S.J. 2005. CD144 (VE-cadherin) is transiently expressed by fetal liver hematopoietic stem cells. *Blood* **106:** 903–905.

Kopp, H.G., Ramos, C.A., and Rafii, S. 2006. Contribution of endothelial progenitors and proangiogenic hematopoietic cells to vascularization of tumor and ischemic tissue. *Curr. Opin. Hematol.* **13:** 175–181.

Laitinen, L., Virtanen, I., and Saxen, L. 1987. Changes in the glycosylation pattern during embryonic development of mouse kidney as revealed with lectin conjugates. *J. Histochem. Cytochem.* **35:** 55–65.

Lampugnani, M.G., Orsenigo, F., Gagliani, M.C., Tacchetti, C., and Dejana, E. 2006. Vascular endothelial cadherin controls VEGFR-2 internalization and signaling from intracellular compartments. *J. Cell Biol.* **174:** 593–604.

Lamszus, K., Brockmann, M.A., Eckerich, C., Bohlen, P., May, C., Mangold, U., Fillbrandt, R., and Westphal, M. 2005. Inhibition of glioblastoma angiogenesis and invasion by combined treatments directed against vascular endothelial growth factor receptor-2, epidermal growth factor receptor, and vascular endothelial-cadherin. *Clin. Cancer Res.* **11:** 4934–4940.

Larrivee, B., Niessen, K., Pollet, I., Corbel, S.Y., Long, M., Rossi, F.M., Olive, P.L., and Karsan, A. 2005. Minimal contribution of marrow-derived endothelial precursors to tumor vasculature. *J. Immunol.* **175:** 2890–2899.

Li, H., Gerald, W.L., and Benezra, R. 2004. Utilization of bone marrow-derived endothelial cell precursors in spontaneous prostate tumors varies with tumor grade. *Cancer Res.* **64:** 6137–6143.

Liao, F., Doody, J.F., Overholser, J., Finnerty, B., Bassi, R., Wu, Y., Dejana, E., Kussie, P., Bohlen, P., and Hicklin, D.J. 2002. Selective targeting of angiogenic tumor vasculature by vascular endothelial-cadherin antibody inhibits tumor growth without affecting vascular permeability. *Cancer Res.* **62:** 2567–2575.

Lin, E.Y., Nguyen, A.V., Russell, R.G., and Pollard, J.W. 2001. Colony-stimulating factor 1 promotes progression of mammary tumors to malignancy. *J. Exp. Med.* **193:** 727–740.

Lin, E.Y., Jones, J.G., Li, P., Zhu, L., Whitney, K.D., Muller, W.J., and Pollard, J.W. 2003. Progression to malignancy in the polyoma middle T oncoprotein mouse breast cancer model provides a reliable model for human diseases. *Am. J. Pathol.* **163:** 2113–2126.

Lyden, D., Hattori, K., Dias, S., Costa, C., Blaikie, P., Butros, L., Chadburn, A., Heissig, B., Marks, W., Witte, L., et al. 2001.

Impaired recruitment of bone-marrow-derived endothelial and hematopoietic precursor cells blocks tumor angiogenesis and growth. *Nat. Med.* **7:** 1194–1201.

Machein, M.R., Renninger, S., de Lima-Hahn, E., and Plate, K.H. 2003. Minor contribution of bone marrow-derived endothelial progenitors to the vascularization of murine gliomas. *Brain Pathol.* **13:** 582–597.

May, C., Doody, J.F., Abdullah, R., Balderes, P., Xu, X., Chen, C.P., Zhu, Z., Shapiro, L., Kussie, P., Hicklin, D.J., et al. 2005. Identification of a transiently exposed VE-cadherin epitope that allows for specific targeting of an antibody to the tumor neovasculature. *Blood* **105:** 4337–4344.

McDevitt, M.R., Ma, D., Lai, L.T., Simon, J., Borchardt, P., Frank, R.K., Wu, K., Pellegrini, V., Curcio, M.J., Miederer, M., et al. 2001. Tumor therapy with targeted atomic nanogenerators. *Science* **294:** 1537–1540.

McDevitt, M.R., Ma, D., Simon, J., Frank, R.K., and Scheinberg, D.A. 2002. Design and synthesis of ^{225}Ac radioimmunopharmaceuticals. *Appl. Radiat. Isot.* **57:** 841–847.

Minami, E., Laflamme, M.A., Saffitz, J.E., and Murry, C.E. 2005. Extracardiac progenitor cells repopulate most major cell types in the transplanted human heart. *Circulation* **112:** 2951–2958.

Nozawa, H., Chiu, C., and Hanahan, D. 2006. Infiltrating neutrophils mediate the initial angiogenic switch in a mouse model of multistage carcinogenesis. *Proc. Natl. Acad. Sci.* **103:** 12493–12498.

Peichev, M., Naiyer, A.J., Pereira, D., Zhu, Z., Lane, W.J., Williams, M., Oz, M.C., Hicklin, D.J., Witte, L., Moore, M.A., et al. 2000. Expression of VEGFR-2 and AC133 by circulating human CD34$^+$ cells identifies a population of functional endothelial precursors. *Blood* **95:** 952–958.

Perfetto, S.P., Chattopadhyay, P.K., and Roederer, M. 2004. Seventeen-colour flow cytometry: Unravelling the immune system. *Nat. Rev. Immunol.* **4:** 648–655.

Peters, B.A., Diaz, L.A., Polyak, K., Meszler, L., Romans, K., Guinan, E.C., Antin, J.H., Myerson, D., Hamilton, S.R., Vogelstein, B., et al. 2005. Contribution of bone marrow-derived endothelial cells to human tumor vasculature. *Nat. Med.* **11:** 261–262.

Pollard, J.W. 2004. Tumour-educated macrophages promote tumour progression and metastasis. *Nat. Rev. Cancer* **4:** 71–78.

Rafii, S., Lyden, D., Benezra, R., Hattori, K., and Heissig, B. 2002. Vascular and haematopoietic stem cells: Novel targets for anti-angiogenesis therapy? *Nat. Rev. Cancer* **2:** 826–835.

Rajantie, I., Ilmonen, M., Alminaite, A., Ozerdem, U., Alitalo, K., and Salven, P. 2004. Adult bone marrow-derived cells recruited during angiogenesis comprise precursors for periendothelial vascular mural cells. *Blood* **104:** 2084–2086.

Ribatti, D. 2004. The involvement of endothelial progenitor cells in tumor angiogenesis. *J. Cell. Mol. Med.* **8:** 294–300.

Ruzinova, M.B., Schoer, R.A., Gerald, W., Egan, J.E., Pandolfi, P.P., Rafii, S., Manova, K., Mittal, V., and Benezra, R. 2003. Effect of angiogenesis inhibition by Id loss and the contribution of bone-marrow-derived endothelial cells in spontaneous murine tumors. *Cancer Cell* **4:** 277–289.

Shaked, Y., Ciarrocchi, A., Franco, M., Lee, C.R., Man, S., Cheung, A.M., Hicklin, D.J., Chaplin, D., Foster, F.S., Benezra, R., et al. 2006. Therapy-induced acute recruitment of circulating endothelial progenitor cells to tumors. *Science* **313:** 1785–1787.

Song, S., Ewald, A.J., Stallcup, W., Werb, Z., and Bergers, G. 2005. PDGFRβ$^+$ perivascular progenitor cells in tumours regulate pericyte differentiation and vascular survival. *Nat. Cell Biol.* **7:** 870–879.

Spring, H., Schuler, T., Arnold, B., Hammerling, G.J., and Ganss, R. 2005. Chemokines direct endothelial progenitors into tumor neovessels. *Proc. Natl. Acad. Sci.* **102:** 18111–18116.

Tudor, K.S., Deem, T.L., and Cook-Mills, J.M. 2000. Novel α 4-integrin ligands on an endothelial cell line. *Biochem. Cell Biol.* **78:** 99–113.

Urbich, C. and Dimmeler, S. 2004. Endothelial progenitor cells functional characterization. *Trends Cardiovasc. Med.* **14:** 318–322.

Voswinckel, R., Ziegelhoeffer, T., Heil, M., Kostin, S., Breier, G., Mehling, T., Haberberger, R., Clauss, M., Gaumann, A., Schaper, W., et al. 2003. Circulating vascular progenitor cells do not contribute to compensatory lung growth. *Circ. Res.* **93:** 372–379.

Xiao, K., Allison, D.F., Kottke, M.D., Summers, S., Sorescu, G.P., Faundez, V., and Kowalczyk, A.P. 2003. Mechanisms of VE-cadherin processing and degradation in microvascular endothelial cells. *J. Biol. Chem.* **278:** 19199–19208.

Ziegelhoeffer, T., Fernandez, B., Kostin, S., Heil, M., Voswinckel, R., Helisch, A., and Schaper, W. 2004. Bone marrow-derived cells do not incorporate into the adult growing vasculature. *Circ. Res.* **94:** 230–238.